

An Orally Applicable Shiga Toxin Neutralizer Functions in the Intestine To Inhibit the Intracellular Transport of the Toxin[▽]

Miho Watanabe-Takahashi,¹ Toshio Sato,² Taeko Dohi,³ Noriko Noguchi,⁴ Fumi Kano,^{5,6}
Masayuki Murata,⁵ Takashi Hamabata,² Yasuhiro Natori,⁷ and Kiyotaka Nishikawa^{1*}

Department of Molecular Life Sciences, Faculty of Life and Medical Sciences, Doshisha University, Kyoto, Japan¹; Department of Infectious Disease, Research Institute, International Medical Center of Japan, Tokyo, Japan²; Department of Gastroenterology, Research Institute, International Medical Center of Japan, Tokyo, Japan³; Department of Systems Life Sciences, Faculty of Life and Medical Sciences, Doshisha University, Kyoto, Japan⁴; Department of Life Sciences, Graduate School of Arts and Sciences, The University of Tokyo, Tokyo, Japan⁵; PRESTO, Japan Science and Technology Agent, Saitama, Japan⁶; and Department of Health Chemistry, School of Pharmacy, Iwate Medical University, Iwate, Japan⁷

Received 8 September 2009/Returned for modification 4 October 2009/Accepted 20 October 2009

Shiga toxin 2 (Stx2) is a major virulence factor in infections with Stx-producing *Escherichia coli* (STEC), which causes gastrointestinal diseases and sometimes fatal systemic complications. Recently, we developed an oral Stx2 inhibitor known as Ac-PPP-tet that exhibits remarkable therapeutic potency in an STEC infection model. However, the precise mechanism underlying the in vivo therapeutic effects of Ac-PPP-tet is unknown. Here, we found that Ac-PPP-tet completely inhibited fluid accumulation in the rabbit ileum caused by the direct injection of Stx2. Interestingly, Ac-PPP-tet accumulated in the ileal epithelial cells only through its formation of a complex with Stx2. The formation of Ac-PPP-tet–Stx2 complexes in cultured epithelial cells blocked the intracellular transport of Stx2 from the Golgi apparatus to the endoplasmic reticulum, a process that is essential for Stx2 cytotoxicity. Thus, Ac-PPP-tet is the first Stx neutralizer that functions in the intestine by altering the intracellular transport of Stx2 in epithelial cells.

Infection with Shiga toxin (Stx)-producing *Escherichia coli* (STEC) in humans causes gastrointestinal diseases that are often followed by potentially fatal systemic complications such as acute encephalopathy and hemolytic-uremic syndrome (12, 22, 25, 26). Stx is produced in the gut, traverses the epithelium, and passes into the circulation. Circulating Stx then causes vascular damage in specific target tissues such as the brain and the kidney, resulting in systemic complications. For this reason, development of a neutralizer that specifically binds to and inhibits Stx in the gut and/or in the circulation would be a promising therapeutic approach.

Stx is classified into two subgroups, Stx1 and Stx2. Stx2 is more closely related to the severity of STEC infections than Stx1 (6, 23, 31, 33). Stx consists of a catalytic A subunit and a pentameric B subunit. The former has 28S rRNA *N*-glycosidase activity and inhibits eukaryotic protein synthesis, while the latter is responsible for binding to the functional cell surface receptor Gb3 [Gal α (1-4)-Gal β (1-4)-Glc β 1-ceramide] (11, 17, 25). The crystal structure of Stx reveals the presence of three distinctive binding sites (i.e., sites 1, 2, and 3) on each B subunit monomer for the trisaccharide moiety of Gb3 (7, 16). Highly selective and potent binding of Stx to Gb3 is attributed mainly to the multivalent interaction between the B subunit pentamer and the trisaccharide. This so-called clustering effect has formed the basis for the development of several synthetic Stx neutralizers that contain the trisaccharide in multiple con-

figurations (3, 5, 14, 18, 19, 36). These neutralizers can strongly bind to Stx and inhibit its cytotoxic activity. Some are also effective in STEC infection models (18, 19, 36). However, the clinical application of these neutralizers has been substantially hampered by the synthetic complexity of the trisaccharide moiety.

We have recently screened a library of novel tetravalent peptides that exert a clustering effect and have identified four peptide motifs that are superior to trisaccharide in binding Stx (20). Tetravalent forms of these peptides bind with high affinity to one trisaccharide-binding site (site 3) of Stx2 and effectively inhibit Stx2 cytotoxicity. This is particularly true of the neutralizer designated PPP-tet, which contains four Pro-Pro-Arg-Arg-Arg-Arg motifs. PPP-tet protects mice from a fatal dose of *E. coli* O157:H7, even when the peptide is orally administered after the establishment of infection (20). Moreover, the addition of acetyl groups to all the amino termini of PPP-tet (yielding Ac-PPP-tet) makes this compound resistant to proteolysis and markedly enhances its protective activity against STEC infection, indicating that Ac-PPP-tet holds promise as a therapeutic agent for STEC infections.

After binding to Gb3, Stx is first transported to the Golgi apparatus in a retrograde manner and then transported to the endoplasmic reticulum (ER). On the other hand, the Stx catalytic A subunit is released into the cytoplasm, where it inhibits protein synthesis (27, 29). The retrograde transport of Stx is known to be essential for Stx cytotoxicity (2, 27, 28). In Vero cells, one of the cell types most sensitive to Stx, PPP-tet prevents Stx2 cytotoxicity by inducing the aberrant transport of Stx from the Golgi apparatus to an acidic compartment rather than to the ER, leading to the degradation of Stx (20). An advantage of PPP-tet is its ability to partially permeate cells,

* Corresponding author. Mailing address: Department of Molecular Life Sciences, Faculty of Life and Medical Sciences, Doshisha University, 1-3 Miyakotani, Tatara, Kyotanabe, Kyoto 610-0321, Japan. Phone and fax: (81) 774-65-6471. E-mail: knishika@mail.doshisha.ac.jp.

[▽] Published ahead of print on 26 October 2009.

which allows it to inhibit the cytotoxicity of Stx2 already incorporated into cells (20). Nevertheless, the precise mechanism by which PPP-tet and Ac-PPP-tet function in vivo, as well as the identities of the organs or cells targeted by these compounds, is unknown.

To understand how orally administered Ac-PPP-tet functions in vivo, we investigated the effect of Ac-PPP-tet on fluid accumulation in the rabbit ileum caused by the direct injection of Stx2. The rabbit ileal loop system is highly valid for evaluating the toxicity of Stx2 produced in the intestine after infection. We also examined the localization of the tetravalent peptide and Stx2 in the intact rabbit ileum, cultured ileal specimens, and Caco-2 intestinal epithelial cells. Our results reveal that Ac-PPP-tet functions as a potent Stx2 neutralizer in the intestine by altering the intracellular transport of Stx2 in epithelial cells.

MATERIALS AND METHODS

Materials. Recombinant Stx2 (21) and cholera toxin (34) were prepared according to published methods. Ac-PPP-tet and biotin-PPP-tet were prepared as described previously (20). Streptavidin-Alexa 488 was obtained from Invitrogen (Carlsbad, CA). Anti-Stx1 and anti-Stx2 mouse monoclonal IgG was obtained from Toxin Technology, Inc. (Sarasota, FL). Japanese white rabbits were obtained from Japan SLC (Shizuoka, Japan). The WST-1 cell counting kit was obtained from Wako Pure Industries (Osaka, Japan). Mouse anti-GM130 IgG monoclonal antibody was purchased from BD Biosciences Pharmingen (San Diego, CA), and mouse anti-Hsp47 monoclonal antibody was purchased from StressGen (San Diego, CA). Rabbit anti-Stx2 antiserum was provided by S. Yamasaki (Osaka Prefecture University, Japan). Stx2 conjugated with Alexa Fluor 488 at the amino groups, as well as Ac-PPP-tet conjugated with Alexa Fluor 555 at the single carboxyl group, was prepared using the Alexa Fluor protein-labeling kit (Invitrogen).

Cell culture. Caco-2 cells were obtained from the American Type Culture Collection (Manassas, VA) and were maintained in Dulbecco's modified essential medium (Invitrogen) supplemented with 10% fetal bovine serum, 100 U/ml penicillin, 100 µg/ml streptomycin, and 25 µg/ml amphotericin B. Caco-2 cells were plated at a density of approximately 10^5 cells/ml, grown to confluence for 3 days, treated with 2 mM butyric acid sodium salt for 4 days, and then used for experiments.

Measurement of fluid accumulation. Fluid accumulation induced by Stx2 in rabbit ileal loops was examined as described previously (8, 9). Conventional Japanese white rabbits (1.5 to 2 kg) were subjected to fasting for 18 h before surgery. Rabbits were anesthetized with thiopental sodium, and the intestines were exteriorized through a midline incision. In each loop, 8 to 10 segments (about 10 cm each) were ligated. One milliliter of saline or a solution of Stx2 (10 µg/ml saline) and a dose of the peptide compound were simultaneously injected into the loop. Cholera toxin (500 ng/ml saline in a 1-ml volume) served as a positive control. Eighteen hours after injection, rabbits were killed and the loops were excised. The ratio of the weight of the fluid-containing loop to the length of the loop (the fluid accumulation ratio, expressed in grams per centimeter) was calculated.

Intestinal histopathology. A portion of the ileal loop prepared as described above was removed, washed with cold phosphate-buffered saline (PBS), and immediately fixed with 4% paraformaldehyde in PBS. The tissue was then embedded in paraffin, sectioned, and stained with hematoxylin and eosin.

Preparation of freshly isolated ileal blocks. Fasting rabbits were anesthetized, and the ilea were exteriorized as described above. Small blocks (about 0.8 by 0.8 by 0.2 cm) containing the intestinal villi were collected from the ilea, washed with PBS, and cultured in a 24-well plate in Dulbecco's modified essential medium supplemented with 10% fetal bovine serum. After a 1-h incubation of the blocks with Stx2 (10 µg/ml) and/or biotin-PPP-tet (1.4 mM), the blocks were fixed with 4% paraformaldehyde, embedded in paraffin, and sectioned. The sections were then stained with hematoxylin and eosin.

Localization of biotin-PPP-tet in the ileum. Sections obtained from the embedded specimens were deparaffinized, and the endogenous peroxidase activities were blocked by incubating sections in a hydrogen peroxide solution for 20 min. Biotin-PPP-tet was detected with streptavidin-Alexa 488.

Immunocytochemical staining. Sections prepared from ileal blocks were deparaffinized, and endogenous peroxidase activities were blocked with a 20-min incubation in a hydrogen peroxide solution. For Stx2 immunostaining, sections were treated with blockase (DS Pharma Biomedical Co., Ltd., Osaka, Japan) for 30 min and then incubated with mouse monoclonal anti-Stx IgG (1 µg/ml) for 3 h at room temperature. The sections were then treated with anti-mouse IgG-tetramethyl rhodamine isocyanate for 1.5 h at room temperature.

Cytotoxicity assay. Caco-2 cells grown in a 96-well plate were treated with Stx2 (100 pg/ml) in the absence or presence of Ac-PPP-tet for 48 h. The relative number of living cells was then determined using a WST-1 cell counting kit according to the manufacturer's instructions.

Intracellular localization of Stx2 and Ac-PPP-tet. Caco-2 cells grown in a glass-base dish (35 mm in diameter) were treated with Alexa Fluor 488-labeled Stx2 (1 µg/ml) in the absence or presence of Alexa Fluor 555-labeled Ac-PPP-tet (16 µM) for 1 h at 4°C. The cells were then washed, incubated for the indicated time at 37°C, and analyzed by confocal laser scanning microscopy with an instrument from Olympus (Melville, NY). To examine the colocalization of Stx2 with a Golgi apparatus marker or an ER marker, we exposed Caco-2 cells to Stx2 (1 µg/ml) in the absence or presence of Ac-PPP-tet (49 µM) for 1 h at 37°C and then fixed the cells with 3% paraformaldehyde. Stx2 immunostaining was carried out by successively incubating cells with rabbit anti-Stx2 polyclonal antibody and Alexa Fluor 488-labeled goat anti-rabbit IgG. Immunostaining for GM130, a Golgi apparatus marker, was performed using mouse anti-GM130 IgG monoclonal antibody and Alexa Fluor 546-labeled goat anti-mouse IgG. Immunostaining for Hsp47, an ER marker, was performed using mouse anti-Hsp47 monoclonal antibody and Alexa Fluor 546-labeled goat anti-mouse IgG.

To examine the complex formation by Ac-PPP-tet and Stx2 in Caco-2 cells, the cells were treated with Alexa Fluor 555-labeled Ac-PPP-tet (16 µM) for 30 min at 37°C. The cells were then washed and further incubated for 30 min at 37°C. The cells were cultured for 30 min in the presence or absence of Alexa Fluor 488-labeled Stx2 (1 µg/ml) and analyzed by confocal scanning microscopy.

RESULTS

Tetravalent peptides inhibit Stx2-induced fluid accumulation in the rabbit ileum. First, we examined the effect of Ac-PPP-tet (Fig. 1A) on fluid accumulation in the rabbit ileal loop caused by the direct injection of Stx2. Treatment with Stx2 induced marked fluid accumulation and bleeding, both of which reflect toxicity to ileum epithelial cells (Fig. 1B and C). The positive control, cholera toxin, also induced fluid accumulation. Coadministration of a high dose of Ac-PPP-tet (1.6 or 4.9 µmol) with Stx2 completely inhibited fluid accumulation, though coadministration of a low dose of Ac-PPP-tet (0.16 or 0.49 µmol) had less effect (Fig. 1B, C, and D). Biotin-PPP-tet had an inhibitory effect similar to that of Ac-PPP-tet (Fig. 1C), showing that biotin substitution for the acetyl groups at the amino termini of the tetravalent peptide does not alter activity against Stx2. Fluid accumulation levels in ileal segments treated with saline and those treated with either tetravalent peptide alone were comparable.

Histological analyses were performed on the ileum specimens used as described above to determine the effect of Ac-PPP-tet or biotin-PPP-tet on Stx2-induced pathological changes. Stx2 treatment was associated with severe ileal damage, particularly the extensive loss and degeneration of intestinal villi. Consistent with the ability of the tetravalent peptides to inhibit fluid accumulation, coadministration of Ac-PPP-tet or biotin-PPP-tet with Stx2 markedly reduced this damage (Fig. 2A). No damage was observed in ileal segments treated with saline or either tetravalent peptide alone (data not shown).

Analysis of the localization of biotin-PPP-tet by using streptavidin-Alexa 488 revealed that, in the presence of Stx2, biotin-PPP-tet efficiently accumulated mainly in the ileal epi-

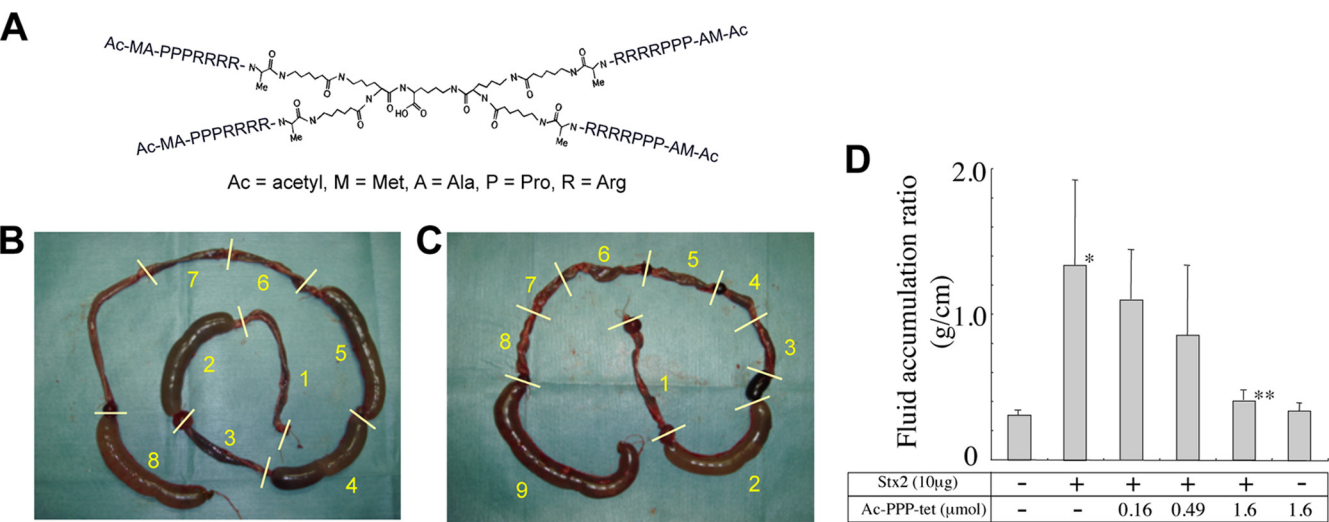


FIG. 1. Tetravalent peptides inhibit Stx2-induced fluid accumulation in the rabbit ileal loop. (A) Structure of Ac-PPP-tet. Me, methyl. (B and C) Ileal loops were treated as indicated below and were excised after 18 h. (B) Segment treatments: 1, saline; 2, Stx2 (10 μ g); 3, Stx2 (10 μ g) and Ac-PPP-tet (1.6 μ mol); 4, Stx2 (10 μ g) and Ac-PPP-tet (0.49 μ mol); 5, Stx2 (10 μ g) and Ac-PPP-tet (0.16 μ mol); 6, Ac-PPP-tet (1.6 μ mol); 7, saline; and 8, cholera toxin (500 ng). (C) Segment treatments: 1, saline; 2, Stx2 (10 μ g); 3, Stx2 (10 μ g) and Ac-PPP-tet (1.6 μ mol); 4, Stx2 (10 μ g) and Ac-PPP-tet (4.9 μ mol); 5, Ac-PPP-tet (1.6 μ mol); 6, Stx2 (10 μ g) and biotin-PPP-tet (1.4 μ mol); 7, Stx2 (10 μ g) and biotin-PPP-tet (4.3 μ mol); 8, biotin-PPP-tet (1.4 μ mol); and 9, cholera toxin (500 ng). (D) Effect of Ac-PPP-tet on Stx2-induced fluid accumulation in ileal loops. Ileal loops were treated as indicated, and fluid accumulation ratios were determined. Values are means \pm standard errors of three determinations. *, $P < 0.01$ for comparison to control, and **, $P < 0.05$ for comparison to treatment with Stx2 alone by an unpaired t test.

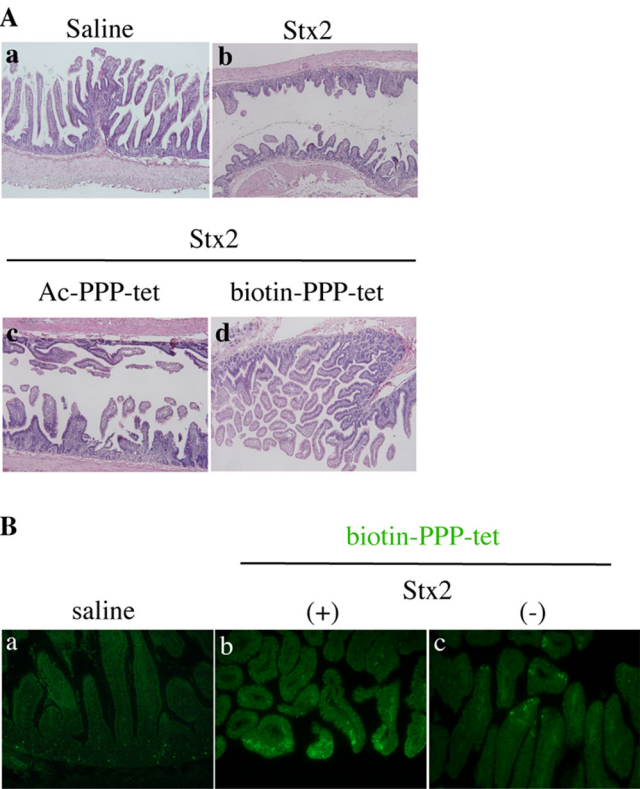


FIG. 2. Effect of Ac-PPP-tet on Stx2-induced ileal damage. (A) Hematoxylin and eosin staining of sections from the ileal loop subjected to the following treatments: a, saline; b, Stx2 (10 μ g); c, Stx2 (10 μ g) and Ac-PPP-tet (1.6 μ mol); and d, Stx2 (10 μ g) and biotin-PPP-tet (1.4 μ mol). (B) Localization of biotin-PPP-tet in the ileal mucosa by using streptavidin-Alexa 488. The ileal loop was subjected to the following treatments: a, saline; b, Stx2 (10 μ g) and biotin-PPP-tet (1.4 μ mol); and c, biotin-PPP-tet (1.4 μ mol).

thelial cells rather than in the lamina propria. Much less accumulation of biotin-PPP-tet was observed in the absence of Stx2 (Fig. 2B). Previous in vitro studies by our laboratory have shown that both Ac-PPP-tet and biotin-PPP-tet (data not shown) form complexes with Stx2 and that these complexes are incorporated into Vero cells (20). This finding, taken with the present results, suggests that in the ileum the tetravalent peptides and Stx2 form complexes that are incorporated into and accumulate in ileal epithelial cells.

Tetravalent peptides accumulate in ileal epithelial cells only in the presence of Stx2. To understand whether tetravalent peptides may form complexes with Stx2 in ileal epithelial cells, we investigated the colocalization of biotin-PPP-tet and Stx2 by using freshly isolated ileum blocks cultured in medium. After a 1-h incubation of the ileum blocks with Stx2, no pathological changes were observed (Fig. 3A), indicating that this incubation time is suitable for examining the distribution of Stx2 in tissues in the absence of any tissue damage. A 1-h incubation with biotin-PPP-tet and Stx2, but not biotin-PPP-tet alone, induced marked accumulation of the peptide in ileal epithelial cells (Fig. 3B), consistent with the Stx2-dependent accumulation of biotin-PPP-tet in the ileum described above. Immunohistochemical analysis using a Stx2-specific antibody confirmed that, after this time, Stx2 was incorporated into the villi, primarily the ileal epithelial cells lining the villi (Fig. 3C, panels a and b). In blocks treated with Stx2 and biotin-PPP-tet, the localization pattern of Stx2 merged well with that of biotin-PPP-tet, suggesting that tetravalent peptides do in fact form complexes with Stx2 in ileal epithelial cells (Fig. 3C, panel c).

Tetravalent peptides inhibit Stx2 cytotoxicity by inducing aberrant cellular transport of Stx2 in epithelial cells. To determine the precise mechanism by which tetravalent peptides

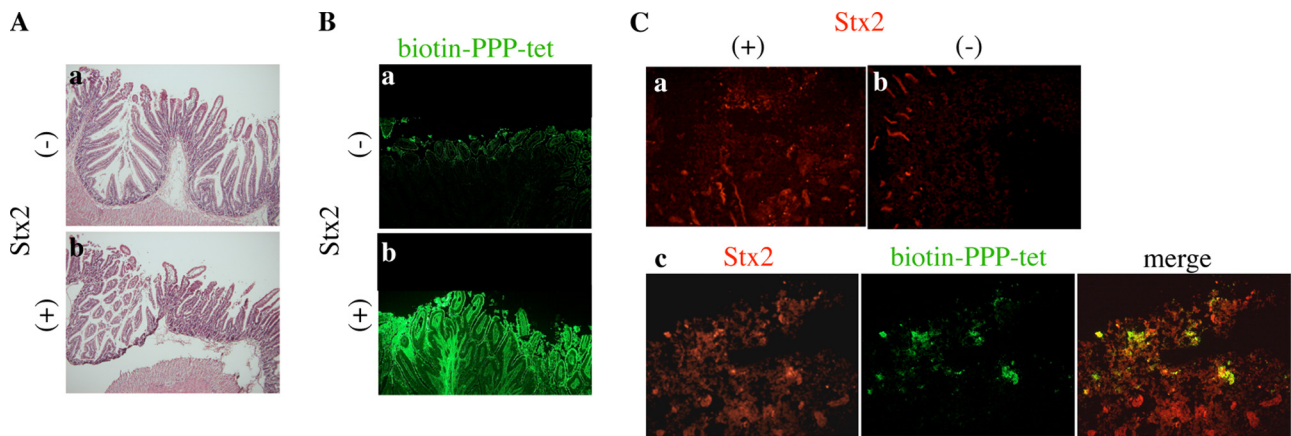


FIG. 3. Tetraivalent peptides accumulate in the ileal epithelial cells in a complex with Stx2. (A) Hematoxylin and eosin staining of sections obtained from the ileal blocks. The blocks were treated with PBS (a) or Stx2 (10 $\mu\text{g/ml}$) (b) for 1 h. (B) Localization of biotin-PPP-tet by using streptavidin-Alexa 488. The block was treated with PBS (a) or Stx2 (10 $\mu\text{g/ml}$) (b) in the presence of biotin-PPP-tet (1.4 mM) for 1 h. (C) Colocalization of Stx2 and biotin-PPP-tet by using anti-Stx monoclonal antibody and streptavidin-Alexa 488. Images show blocks treated with Stx2 (10 $\mu\text{g/ml}$) (a) and PBS (b), as well as blocks treated with Stx2 (10 $\mu\text{g/ml}$) plus biotin-PPP-tet (1.4 mM) (c).

inhibit Stx2 cytotoxicity in ileal epithelial cells, we examined the effects of the peptides on the intracellular transport of the toxin by using Caco-2 cells, a human colon epithelial cell line. As shown in Fig. 4, Ac-PPP-tet efficiently protected Caco-2 cells against the cytotoxic effects of 100 $\mu\text{g/ml}$ Stx2, which resulted in 50% cell viability after a 2-day incubation. Biotin-PPP-tet had a dose-dependent protective effect almost identical to that of Ac-PPP-tet (data not shown). Next, we analyzed the intracellular localization of Alexa Fluor 488-labeled Stx2 after its binding to the surface receptor on Caco-2 cells. Time-

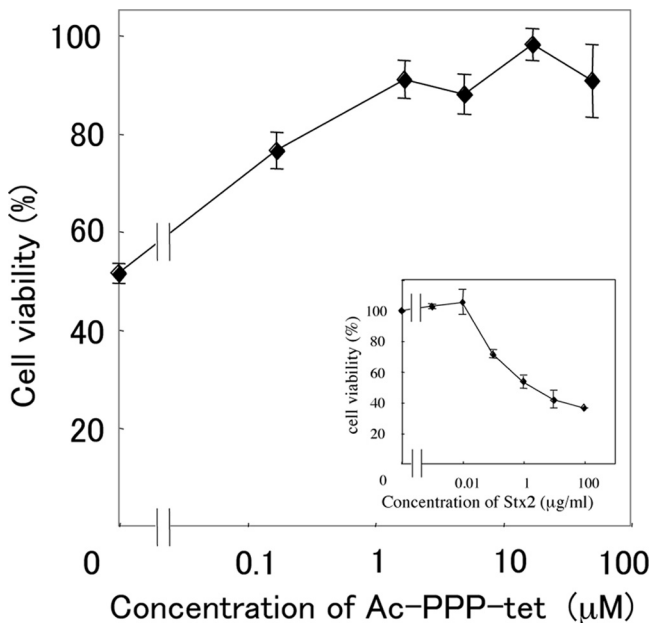


FIG. 4. Tetraivalent peptides inhibit Stx2 cytotoxicity in Caco-2 cells. Caco-2 cells were treated with Stx2 (100 $\mu\text{g/ml}$) in the presence of Ac-PPP-tet for 48 h, and cell viability was determined. The inset shows the dose-dependent effects of Stx2 on Caco-2 cell viability. Data are expressed as percentages (means \pm standard errors; $n = 3$) of the control value.

dependent localization of Stx2 to the Golgi apparatus was confirmed by colocalization with the Golgi apparatus marker GM130 (Fig. 5B). This localization pattern merged well with that of Alexa Fluor 555-labeled Ac-PPP-tet (Fig. 5A), suggesting that the peptide forms a complex with Stx2 and that this complex is then incorporated into the cells and transferred to the Golgi apparatus. In contrast, colocalization of Stx2 with the ER marker Hsp47 was completely inhibited by the presence of Ac-PPP-tet (Fig. 5C), indicating that the transport of Stx2 from the Golgi apparatus to the ER was specifically blocked by the presence of Ac-PPP-tet.

In order to further confirm the above conclusion, we examined whether Ac-PPP-tet could directly interact with Stx2 in living cells. After treatment of Caco-2 cells with Alexa Fluor 555-labeled Ac-PPP-tet, Ac-PPP-tet was substantially incorporated into and diffusely distributed in the cells. Following the addition of Alexa Fluor 488-labeled Stx2, Ac-PPP-tet was dynamically redistributed to the Golgi region, where it colocalized with Stx2 (Fig. 6). Such movement of Ac-PPP-tet was not observed in the absence of Stx2. These results indicate that Ac-PPP-tet can directly bind to Stx2 in living cells and that Stx2 is then transferred to the Golgi apparatus in a complex with Ac-PPP-tet.

DISCUSSION

In the present study, we found that Ac-PPP-tet completely inhibited fluid accumulation and tissue damage in the rabbit ileum caused by the direct injection of Stx2 when Ac-PPP-tet and the toxin were administered simultaneously. Since the rabbit ileal loop system is highly suitable for evaluating the direct toxicity of Stx2 in intestinal epithelial cells, our finding clearly demonstrates that Ac-PPP-tet functions to protect epithelial cells from damage caused by the toxin. Our findings also suggest that the tetraivalent peptide accumulates in ileal epithelial cells only through the formation of a complex with Stx2. Thus, the mechanism of action of Ac-PPP-tet is likely to be different from that of other Stx neutralizers previously

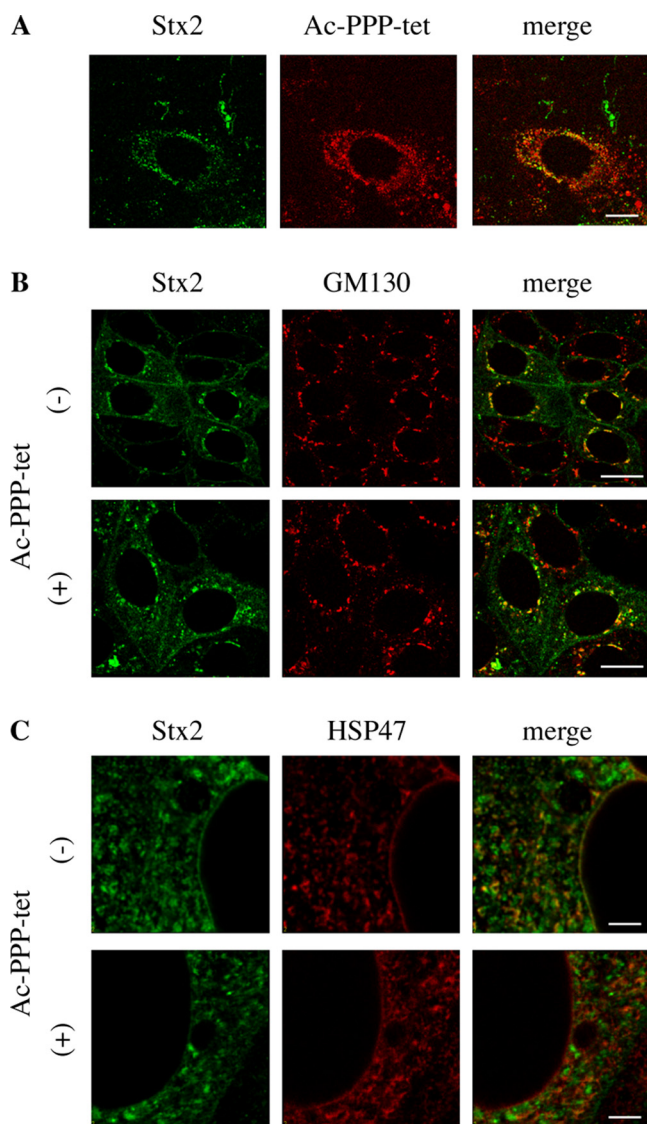


FIG. 5. Tetraivalent peptides induce aberrant cellular transport of Stx2 in Caco-2 cells. (A) Confocal images of the intracellular localization patterns of Alexa Fluor 488-labeled Stx2 (1 μg/ml) in the presence of Alexa Fluor 555-labeled Ac-PPP-tet (16 μM). The bar indicates 20 μm. (B) Immunocytochemical analysis of the colocalization of Stx2 (1 μg/ml) with GM130 in the presence or absence of Ac-PPP-tet (49 μM). The bars indicate 20 μm. (C) Immunocytochemical analysis of the colocalization of Stx2 (1 μg/ml) with Hsp47 in the presence or absence of Ac-PPP-tet (49 μM). The bars indicate 5 μm.

shown to function in the intestinal tract, all of which exert their inhibitory effects by binding to the toxin and inhibiting its incorporation into the epithelial cells (24, 35, 36). In Caco-2 cells, the formation of complexes of Ac-PPP-tet and Stx2 blocked the intracellular transport of Stx2 from the Golgi apparatus to the ER, probably resulting in the efficient degradation of this toxin. Thus, Ac-PPP-tet appears to function in the intestine by affecting the intracellular transport of Stx2, confirming the crucial role of this transport system in vivo, especially in the intestinal epithelial cells.

In mice, Ac-PPP-tet offers remarkable protection against the

lethality of *E. coli* O157:H7 infection when the peptide is administered intragastrically beginning on day 2 of infection (20). Interestingly, Stx was undetectable in sera from Ac-PPP-tet-treated mice on day 3 of infection, when serum Stx concentrations in untreated mice peaked (data not shown) (15). The molecular basis of this phenomenon is unclear, though the present findings suggest that intragastrically administered Ac-PPP-tet induces detoxification of Stx2 in the intestinal epithelial cells and, consequently, prevents its intrusion into the circulation. We have found that direct administration of Ac-PPP-tet into the circulation with Stx2 does not rescue mice from lethality (K. Nishikawa et al., unpublished data), supporting the notion that orally administered Ac-PPP-tet detoxifies Stx2 in the intestine but not in the circulation.

In Caco-2 cells, both Stx1 and Stx2 are transported to the ER along the retrograde pathway and inhibit protein synthesis (30). Stx1 is also able to translocate across the apical side of the intestinal epithelial monolayer to the basolateral side in a Gb3-independent manner. The ability of Stx2 to perform this type of translocation is approximately 10-fold weaker (1, 10). Thus, the fluid accumulation and tissue damage observed in the present study are likely attributable to Stx2, which is transported mainly through the retrograde pathway rather than through transcytosis across intestinal epithelial cells. Moreover, Ac-PPP-tet may protect against the Stx2-induced ileal damage by inhibiting the retrograde transport of the toxin.

We have previously shown that, in Caco-2 cells, the cell binding and retrograde transport of Stx1 and Stx2 are Gb3-dependent events. Specifically, we showed that Stx-stimulated interleukin-8 production, which requires transport of the catalytic A subunit into the cytosol through the retrograde pathway, is markedly inhibited by SUPER TWIGs (37; Nishikawa et al., unpublished), synthetic Stx neutralizers that contain the trisaccharide moiety of Gb3 in multivalent configurations (19). Given that Ac-PPP-tet specifically binds to Stx2 through one of the three trisaccharide-binding sites on the B subunit (site 3), our present observations suggest that the Stx2–Ac-PPP-tet complex binds to cell surface Gb3 through the remaining binding site(s) (i.e., site 1 and/or site 2) and is then transferred to the Golgi apparatus but not to the ER in Caco-2 cells. Taken together, our findings support an essential role for site 3 in the transport of Stx2 from the Golgi apparatus to the ER in the ileal epithelial cells, as has been shown previously for Vero cells (20).

A high-molecular-weight fraction of hop bract extract (HBT), which contains procyanidine polymers, has been shown previously to inhibit the cytotoxic activity of Stx1 in Vero cells and Stx1-induced fluid accumulation in the rabbit ileal loop (32). HBT inhibits the RNA *N*-glycosidase activity of the Stx1 A subunit and then interferes with protein synthesis inhibition, suggesting that the direct target of HBT is the catalytic A subunit of Stx. On the other hand, the Stx2 B subunit has been shown to induce fluid accumulation independently of A subunit activity in rat colon loops by altering the balance of intestinal absorption and secretion toward net secretion (4). Thus, the potent inhibitory effect of Ac-PPP-tet on Stx2-induced fluid accumulation in rabbit ileal loops may be attributable to the unique ability of Ac-PPP-tet to inhibit not only the cytotoxicity of the A subunit by inducing aberrant transport and degradation, but also A subunit-independent intracellular signaling

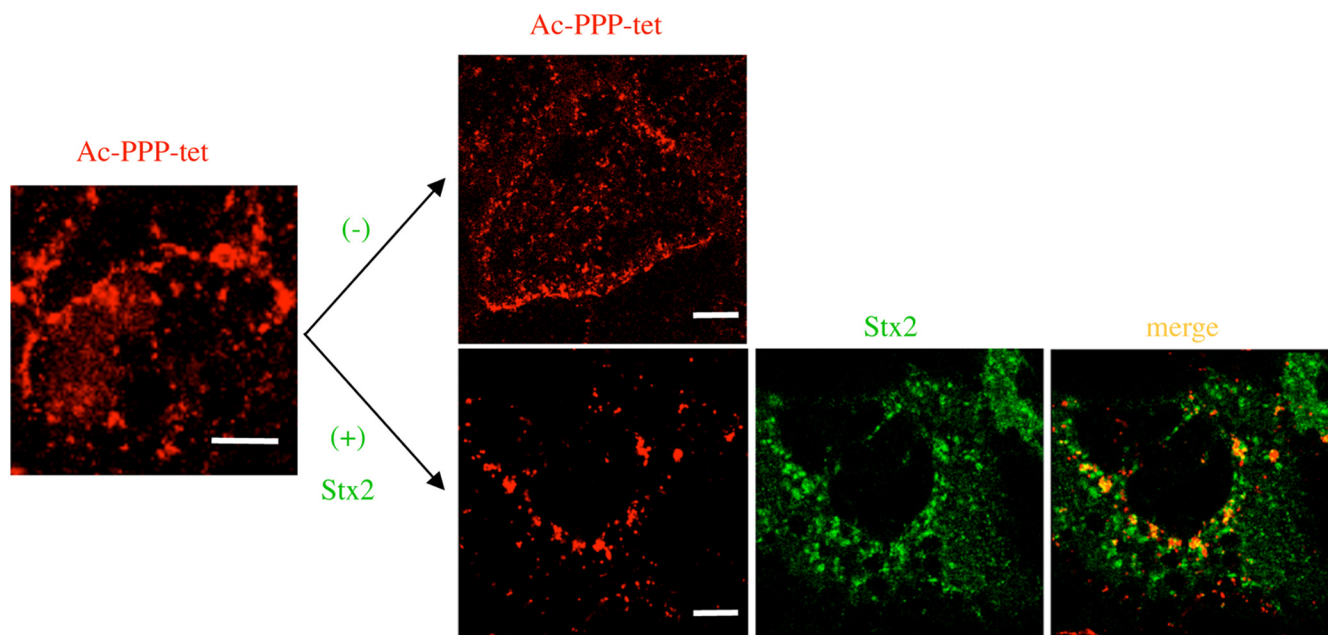


FIG. 6. Complex formation by Ac-PPP-tet and Stx2 in Caco-2 cells. Caco-2 cells that were pretreated with Alexa Fluor 555-labeled Ac-PPP-tet (16 μ M) were cultured for 30 min in the presence or absence of Alexa Fluor 488-labeled Stx2 (1 μ g/ml). Confocal images of the intracellular localization patterns of Ac-PPP-tet and Stx2 are shown. The bars indicate 10 μ m.

activated by the B subunit through binding with Gb3. Previous observations that the protein kinase C inhibitor H-7 and indomethacin inhibit Stx1-induced fluid accumulation in the rabbit ileum without directly affecting the toxin (13) suggest that protein kinase C activation and prostaglandin production participate in signaling downstream of the binding of Stx with Gb3. Similar intracellular signaling events may be blocked by the formation of complexes between Stx2 and Ac-PPP-tet in epithelial cells, although this issue awaits further investigation.

In conclusion, our results suggest that orally administered Ac-PPP-tet accumulates in ileal epithelial cells through the formation of a complex with Stx2. Formation of this complex may specifically block the intracellular transport of Stx2 from the Golgi apparatus to the ER, resulting in the degradation of the toxin and a reduction in its circulating levels. Thus, Ac-PPP-tet appears to function in the intestine by affecting the intracellular transport of Stx2 in the epithelial cells.

ACKNOWLEDGMENTS

We thank Michael Berne (Tufts University) for peptide synthesis.

This study was supported by an International Health Cooperation Research grant (18-C-5) from the Ministry of Health, Labor and Welfare, Japan; a grant from the Fugaku Trust for Medicinal Research; and grants from the Ministry of Education, Culture, Sports, Science and Technology, Japan (an Academic Frontier Research Project grant for the "New Frontier of Biomedical Engineering Research" and scientific research grant no. 19659027).

REFERENCES

1. Acheson, D. W., R. Moore, S. De Breucker, L. Lincicome, M. Jacewicz, E. Skutelsky, and G. T. Keusch. 1996. Translocation of Shiga toxin across polarized intestinal cells in tissue culture. *Infect. Immun.* **64**:3294–3300.
2. Arab, S., and C. A. Lingwood. 1998. Intracellular targeting of the endoplasmic reticulum/nuclear envelope by retrograde transport may determine cell hypersensitivity to verotoxin via globotriaosyl ceramide fatty acid isoform traffic. *J. Cell. Physiol.* **177**:646–660.
3. Armstrong, G. D., E. Fodor, and R. Vanmaele. 1991. Investigation of Shiga-like toxin binding to chemically synthesized oligosaccharide sequences. *J. Infect. Dis.* **164**:1160–1167.
4. Creydt, V. P., M. F. Miyakawa, F. Martín, E. Zotta, C. Silberstein, and C. Ibarra. 2004. The Shiga toxin 2 B subunit inhibits net fluid absorption in human colon and elicits fluid accumulation in rat colon loops. *Braz. J. Med. Biol. Res.* **37**:799–808.
5. Dohi, H., Y. Nishida, M. Mizuno, M. Shinkai, T. Kobayashi, T. Takeda, H. Uzawa, and K. Kobayashi. 1999. Synthesis of an artificial glycoconjugate polymer carrying Pk-antigenic trisaccharide and its potent neutralization activity against Shiga-like toxin. *Bioorg. Med. Chem.* **7**:2053–2062.
6. Donohue-Rolfe, A., I. Kondova, S. Oswald, D. Hutto, and S. Tzipori. 2000. *Escherichia coli* O157:H7 strains that express Shiga toxin (Stx) 2 alone are more neurotropic for gnotobiotic piglets than are isotypes producing only Stx1 or both Stx1 and Stx2. *J. Infect. Dis.* **181**:1825–1829.
7. Fraser, M. E., M. Fujinaga, M. M. Cherney, A. R. Melton-Celsa, E. M. Twiddy, A. D. O'Brien, and M. N. James. 2004. Structure of Shiga toxin type 2 (Stx2) from *Escherichia coli* O157:H7. *J. Biol. Chem.* **279**:27511–27517.
8. Gorbach, S. L., J. G. Banwell, B. D. Chatterjee, B. Jacobs, and R. B. Sack. 1971. Acute undifferentiated human diarrhea in the tropics. I. Alterations in intestinal microflora. *J. Clin. Invest.* **50**:881–889.
9. Hitotsubashi, S., Y. Fujii, H. Yamanaka, and K. Okamoto. 1992. Some properties of purified *Escherichia coli* heat-stable enterotoxin II. *Infect. Immun.* **60**:4468–4474.
10. Hurley, B. P., M. Jacewicz, C. M. Thorpe, L. L. Lincicome, A. J. King, G. T. Keusch, and D. W. Acheson. 1999. Shiga toxins 1 and 2 translocate differently across polarized intestinal epithelial cells. *Infect. Immun.* **67**:6670–6677.
11. Karmali, M. A., M. Petric, C. Lim, P. C. Fleming, G. S. Arbus, and H. Lior. 1985. The association between idiopathic hemolytic uremic syndrome and infection by verotoxin-producing *Escherichia coli*. *J. Infect. Dis.* **151**:775–782.
12. Karmali, M. A., B. T. Steele, M. Petric, and C. Lim. 1983. Sporadic cases of hemolytic uremic syndrome associated with fecal cytotoxin and cytotoxin-producing *Escherichia coli*. *Lancet* **i**:619–620.
13. Kaur, T., S. Singh, M. Verma, and N. K. Ganguly. 1997. Calcium and protein kinase C play a significant role in response to Shigella toxin in rabbit ileum both in vivo and in vitro. *Biochim. Biophys. Acta* **1361**:75–91.
14. Kitov, P. I., J. M. Sadowska, G. Mulvey, G. D. Armstrong, H. Ling, N. S. Pannu, R. J. Read, and D. R. Bundle. 2000. Shiga-like toxins are neutralized by tailored multivalent carbohydrate ligands. *Nature* **403**:669–672.
15. Kurioka, T., Y. Yunou, and E. Kita. 1998. Enhancement of susceptibility to Shiga toxin-producing *Escherichia coli* O157:H7 by protein calorie malnutrition in mice. *Infect. Immun.* **66**:1726–1734.
16. Ling, H., A. Boodhoo, B. Hazes, M. D. Cummings, G. D. Armstrong, J. L. Brunton, and R. J. Read. 1998. Structure of the Shiga-like toxin I B-penta-

- mer complexed with an analogue of its receptor Gb₃. *Biochemistry* **37**:1777–1788.
17. Melton-Celsa, A. R., and A. D. O'Brien. 1998. Structure, biology, and relative toxicity of Shiga toxin family members for cells and animals, p. 121–128. In J. B. Kaper and A. D. O'Brien (ed.), *Escherichia coli* O157:H7 and other Shiga toxin-producing *E. coli* strains. American Society for Microbiology, Washington, DC.
 18. Mulvey, G. L., P. Marcato, P. I. Kitov, J. Sadowska, D. R. Bundle, and G. D. Armstrong. 2003. Assessment in mice of the therapeutic potential of tailored, multivalent Shiga toxin carbohydrate ligands. *J. Infect. Dis.* **187**:640–649.
 19. Nishikawa, K., K. Matsuoka, E. Kita, N. Okabe, M. Mizuguchi, K. Hino, S. Miyazawa, C. Yamasaki, J. Aoki, S. Takashima, Y. Yamakawa, M. Nishijima, D. Terunuma, H. Kuzuhara, and Y. Natori. 2002. A therapeutic agent with oriented carbohydrates for treatment of infections by Shiga toxin-producing *Escherichia coli* O157:H7. *Proc. Natl. Acad. Sci. U. S. A.* **99**:7669–7674.
 20. Nishikawa, K., M. Watanabe, E. Kita, K. Igai, K. Omata, M. B. Yaffe, and Y. Natori. 2006. A multivalent peptide-library approach identifies a novel Shiga toxin-inhibitor that induces aberrant cellular transport of the toxin. *FASEB J.* **20**:2597–2599.
 21. Noda, M., T. Yutsudo, N. Nakabayashi, T. Hirayama, and Y. Takeda. 1987. Purification and some properties of Shiga-like toxin from *Escherichia coli* O157:H7 that is immunologically identical to Shiga toxin. *Microb. Pathog.* **2**:339–349.
 22. O'Brien, A. D., and R. K. Holmes. 1987. Shiga and Shiga-like toxins. *Microbiol. Rev.* **51**:206–220.
 23. Ostroff, S. M., P. I. Tarr, M. A. Neill, J. H. Lewis, N. Hargrett-Bean, and J. M. Kobayashi. 1989. Toxin genotypes and plasmid profiles as determinants of systemic sequelae in *Escherichia coli* O157:H7 infections. *J. Infect. Dis.* **160**:994–998.
 24. Paton, A. W., R. Morona, and J. C. Paton. 2000. A new biological agent for treatment of Shiga toxin-producing *Escherichia coli* infections and dysentery in humans. *Nat. Med.* **6**:265–270.
 25. Paton, J. C., and A. W. Paton. 1998. Pathogenesis and diagnosis of Shiga toxin-producing *Escherichia coli* infections. *Clin. Microbiol. Rev.* **11**:450–479.
 26. Riley, L. W., R. S. Remis, S. D. Helgeson, H. B. McGee, J. G. Wells, B. R. Davis, R. J. Hebert, E. S. Olcott, L. M. Johnson, N. T. Hargrett, P. A. Blake, and M. L. Cohen. 1983. Hemorrhagic colitis associated with a rare *Escherichia coli* serotype. *N. Engl. J. Med.* **308**:681–685.
 27. Sandvig, K., O. Garred, K. Prydz, J. V. Kozlov, S. H. Hansen, and B. van Deurs. 1992. Retrograde transport of endocytosed Shiga toxin to the endoplasmic reticulum. *Nature* **358**:510–512.
 28. Sandvig, K., M. Ryd, O. Garred, E. Schweda, P. K. Holm, and B. van Deurs. 1994. Retrograde transport from the Golgi complex to the ER of both Shiga toxin and the nontoxic Shiga B-fragment is regulated by butyric acid and cAMP. *J. Cell Biol.* **126**:53–64.
 29. Sandvig, K., and B. van Deurs. 2000. Entry of ricin and Shiga toxin into cells: molecular mechanisms and medical perspectives. *EMBO J.* **19**:5943–5950.
 30. Schüller, S., G. Frankel, and A. D. Phillips. 2004. Interaction of Shiga toxin from *Escherichia coli* with human intestinal epithelial cell lines and explants: Stx2 induces epithelial damage in organ culture. *Cell. Microbiol.* **6**:289–301.
 31. Siegler, R. L., T. G. Obrig, T. Pysher, J., V. L. Tesh, N. D. Denkers, and F. B. Taylor. 2003. Response to Shiga toxin 1 and 2 in a baboon model of hemolytic uremic syndrome. *Pediatr. Nephrol.* **18**:92–96.
 32. Tagashira, M., K. Yahiro, N. Morinaga, J. Moss, and M. Noda. 2003. Protection with hop bract polyphenol of mice infected with enterohemorrhagic *Escherichia coli* O157:H7 through inhibition of Shiga toxin-1 toxicity. p. 45–48. In 38th U.S.-Japan Cholera and Other Bacterial Enteric Infections Joint Panel Meeting. U.S. Department of Health and Human Disease, Public Health Service, National Institutes of Health, Bethesda, MD.
 33. Tesh, V. L., J. A. Burris, J. W. Owens, V. M. Gordon, E. A. Wadolkowski, A. D. O'Brien, and J. E. Samuel. 1993. Comparison of the relative toxicities of Shiga-like toxins type I and type II for mice. *Infect. Immun.* **61**:3392–3402.
 34. Uesaka, Y., Y. Otsuka, Z. Lin, S. Yamasaki, J. Yamaoka, H. Kurazono, and Y. Takeda. 1994. Simple method of purification of *Escherichia coli* heat-labile enterotoxin and cholera toxin using immobilized galactose. *Microb. Pathog.* **16**:71–76.
 35. Watanabe, M., K. Igai, K. Matsuoka, A. Miyagawa, T. Watanabe, R. Yanoshita, Y. Samejima, D. Terunuma, Y. Natori, and K. Nishikawa. 2006. Structural analysis of the interaction between Shiga toxin B-subunits and linear polymers bearing clustered globotriose residues. *Infect. Immun.* **74**:1984–1988.
 36. Watanabe, M., K. Matsuoka, E. Kita, K. Igai, N. Higashi, A. Miyagawa, T. Watanabe, R. Yanoshita, Y. Samejima, D. Terunuma, Y. Natori, and K. Nishikawa. 2004. Oral therapeutic agents with highly clustered globotriose for treatment of Shiga toxin-producing *Escherichia coli* infections. *J. Infect. Dis.* **189**:360–368.
 37. Yamasaki, C., Y. Natori, X.-T. Zeng, M. Ohmura, S. Yamasaki, Y. Takeda, and Y. Natori. 1999. Induction of cytokines in a human colon epithelial cell line by Shiga toxin 1 (Stx1) and Stx2 but not by non-toxic mutant Stx1 which lacks N-glycosidase activity. *FEBS Lett.* **442**:231–234.